

Spectroscopic Studies of a High Mach-Number Rotating Plasma Flow

ANDO Akira*, ASHINO Masashi, SAGI Yukiko, INUTAKE Masaaki, HATTORI Kunihiko,
YOSHINUMA Mikiro, IMASAKI Atsushi, TOBARI Hiroyuki and YAGAI Tsuyoshi
Dept. of Electrical Engineering, Tohoku University, Sendai 980-8579, Japan

(Received: 5 December 2000 / Accepted: 27 October 2001)

Abstract

Characteristics of an axially-magnetized rotating plasma are investigated by spectroscopy in the HITOP device of Tohoku University. A He plasma flows out axially and rotates azimuthally near the muzzle region of the MPD arcjet. Flow and rotational velocities and temperature of He ions and atoms are measured by Doppler shift and broadening of the HeII ($\lambda = 468.58\text{nm}$) and HeI ($\lambda = 587.56\text{nm}$) lines. Rotational velocity increases with the increase of axially-applied magnetic field strength and discharge current. As discharge current increases and mass flow rate decreases, the plasma flow velocity increases and T_i increases. Ion acoustic Mach number of the plasma flow also increases, but tends to saturate at near 1. Radial profile of space potential is calculated from the obtained rotational velocity. The potential profile in the core region is parabolic corresponding to the observed rigid-body rotation of the core plasma.

Keywords:

plasma acceleration, plasma rotation, HITOP, MPD arcjet, spectroscopy, supersonic plasma flow, shock wave

1. Introduction

A high beta plasma flow with supersonic velocity is one of the interesting topics in MHD researches. Plasma acceleration in supersonic and super-Alfvénic region has attracted attention in relation to the formation of cosmic jet in astrophysics. It has been proposed that a high beta plasma would be confined stably in high Mach number plasma flow, where the static plasma pressure is balanced with the dynamic pressure of the flow according to Beltrami-Bernoulli's conditions [1].

Characteristics of a supersonic plasma flow has been investigated in MPD (Magneto-Plasma-Dynamic) arcjet plasma. A high power quasi-steady MPD arcjet is operated in the HITOP device of Tohoku University. A plasma in an MPD arcjet is accelerated axially by $J_r \times B_\theta$ force, where J_r is radial discharge current and B_θ is

self-induced azimuthal magnetic field.

It has been proposed and examined experimentally to operate an MPD arcjet with a magnetic field applied externally in the axial direction in order to enhance plasma acceleration performance. There are several acceleration mechanisms to an MPD plasma in an externally-applied magnetic field [2,3].

In an axial magnetic field B_z , interaction between B_z and J_r results in azimuthal electromagnetic force $J_r \times B_z$, which rotates the plasma azimuthally. In a divergent nozzle type of the axial magnetic field, the rotational flow energy is expected to convert to the axial flow energy. In addition, the electron Hall current J_θ interacts with B_r , which arises from the divergent magnetic field. This force also accelerates the plasma in the axial

*Corresponding author's e-mail: akira@ecei.tohoku.ac.jp

direction.

A plasma flow velocity and temperature are very important parameters of an MPD arcjet plasma in order to investigate plasma acceleration mechanism and to obtain a high- β and supersonic plasma flow for several MHD studies.

Purpose of the present work is to clarify acceleration mechanism of the MPD arcjet with an externally-applied magnetic field. Several parameters such as an axial and rotational flow velocities, density and ion/electron temperatures are measured in an axially-magnetized MPD plasma. Dependence on discharge current, mass flow rate and intensity of the applied magnetic field are reported and pressure balance of the rotating plasma flow is investigated in this paper.

2. Experimental Apparatus

Experiments are performed in the HITOP (High density TOhoku Plasma) device of Tohoku University [4,5,6]. The HITOP device consists of a large cylindrical vacuum chamber (diameter $D = 0.8\text{m}$, length $L = 3.3\text{m}$) with eleven large and six small magnetic coils, which can generate a uniform magnetic field up to 0.2T . Various types of magnetic field configurations can be formed by adjusting the coil currents. In the present experiments most measurements have been done in a uniform magnetic field.

The MPD arcjet, which is installed at one end of the HITOP, has a coaxial structure with a center tungsten rod cathode and an annular molybdenum anode. Inner diameter of the anode is 3cm . A quasi-steady discharge continues for 1ms with a pulse forming network (PFN) system and a fast puffing of Helium gas. Maximum discharge current is 10kA with a typical discharge voltage of 200V .

A high density (more than 10^{16}cm^{-3}) plasma is formed in the muzzle region of the MPD arcjet. The plasma is accelerated in the axial (Z -axis) direction by $J_r \times B_\theta$ force, and expands in the large vacuum tank along the field line. Then, a high density, highly ionized plasma flow is produced in the HITOP.

The blow-off plasma characteristics are measured at a muzzle region by a spectrometer with a focal length of 1m . Two He lines, that is, HeI ($\lambda = 587.56\text{nm}$) and HeII ($\lambda = 468.58\text{nm}$), are measured in the present experiments. These line spectra are obtained in every 0.1ms time interval during a shot with the spectral resolution of 0.02nm . The spectroscopy data in this paper are taken at 1ms after the discharge is fired. Line emission from the plasma is viewed through a focusing

lens connected with a optical fiber. The viewing angle can be changed from 90 deg. (perpendicular direction) to 60 deg. (oblique direction) to the plasma flow. Ion temperature T_i and axial flow velocity U_i^z of He ions are calculated from the Doppler line broadening and the Doppler shift of the HeII line spectra, which are measured by viewing the plasma flow obliquely. Those of neutral He atoms, T_a and U_a^z , are also obtained from those of HeI line spectra.

Plasma rotation velocity is measured by viewing the plasma flow perpendicularly near the MPD muzzle. Radial profiles of the velocities, U_i^θ and U_a^θ , are obtained by moving the lens vertically (from $Y = -6\text{cm}$ to $Y = 6\text{cm}$).

Electron temperature and density profiles are measured by movable double- and triple-Langmuir probes. Blow-off plasma characteristics are also measured by other diagnostics, such as a microwave reflectometer, a multi-channel magnetic probe array and a time-of-flight neutral particle energy analyzer in the HITOP device.

3. Experimental Results

Radial profiles of line intensities, rotational velocities and temperatures measured at 3cm downstream from MPD outlet ($Z = 3\text{cm}$) are shown in Fig. 1. Profile of the HeII line intensities is strongly peaked in the discharge region, while that of the HeI line intensities is rather broad.

Rotational velocity of He ions, U_i^θ , increases linearly with the radius in the core region, which indicates that the plasma rotates as a rigid body. The rotational velocity attains its maximum value at a radius which corresponds to the inner radius of the anode. Its angular frequency is $2 \times 10^6\text{rad/sec}$ when $I_d = 8.7\text{kA}$ and $B_z = 0.1\text{T}$. The rotation is in the direction of the azimuthal electromagnetic force $J_r \times B_z$.

Ion temperature T_i obtained from the line broadening of the HeII lines is almost constant at 30eV near the muzzle region. Temperature of the He neutral atoms T_a is about 10eV in the flow core region.

The maximum rotational velocities U_i^θ , U_a^θ and temperatures T_i , T_a are also measured as functions of discharge current I_d , mass flow rate \dot{m} and axial magnetic field strength B_z as shown in Fig. 2. As shown in Fig. 2(a), U_i^θ increases linearly with I_d . T_i also increases linearly with I_d for the smaller values and increases steeply for I_d of more than 7kA . On the other hand, U_a^θ of the neutral atoms is almost independent of I_d . As \dot{m} decreases, U_i^θ and T_i increases as shown in Fig.

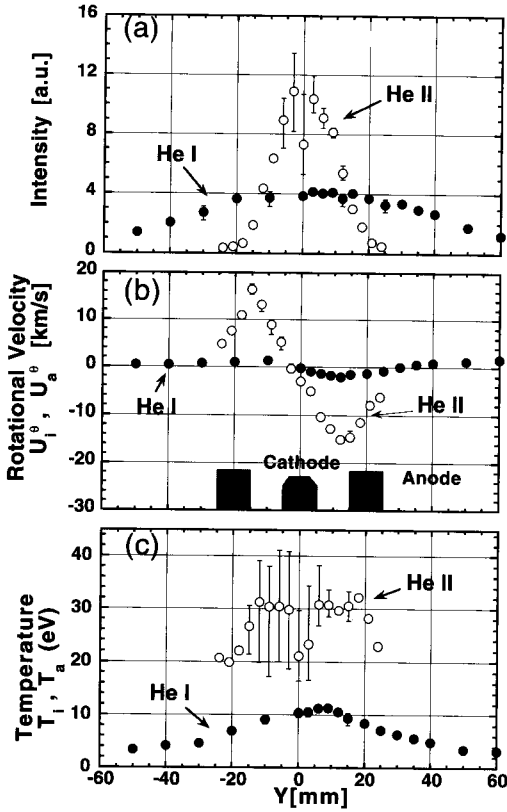


Fig. 1 Radial profiles of (a) spectral line intensity, (b) rotational velocity and (c) temperature. Open and closed circles are those obtained from HeII and HeI lines, respectively. $I_d = 8.7 \text{ kA}$, $\dot{m} = 0.06 \text{ g/sec}$, $B_z = 0.17$.

2(b). The large increase in T_i is also observed for lower \dot{m} . Dependence of U_a^θ and T_a on \dot{m} is quite different from those of U_i^θ and T_i . This discrepancy is probably caused by the decrease in collisional interaction between He ions and atoms for low \dot{m} case. It is noted that U_i^θ increases with an increase of B_z as shown in Fig. 2(c). This corresponds to the azimuthal acceleration by $J_r \times B_z$.

Axial flow velocities U_i^z , U_a^z and temperatures T_i , T_a are measured at $Z = 40 \text{ cm}$ as functions of I_d , \dot{m} and B_z and are shown in Fig. 3. Dependence on I_d and \dot{m} are very similar to those in Fig. 2. On the other hand, the uniform axial magnetic field strength does not affect the axial flow velocity. U_i^z is almost constant as B_z increases, though T_i increases with the increase in B_z , as shown in Fig. 3(c).

Assuming that the axial velocity does not change in the two different measurement position, we can calculate the total velocity U_i^t of He ions by using the obtained data of U_i^z and U_i^θ as

$$U_i^t = \sqrt{(U_i^z)^2 + (U_i^\theta)^2} \quad (1)$$

Then total Mach number M_i^t is expressed as

$$M_i^t = \frac{U_i^t}{C_s} = \frac{U_i^t}{\sqrt{(T_e + T_i) / m_i}} \quad (2)$$

Figure 4 shows dependence of the calculated U_i^t and M_i^t on I_d and \dot{m} . It is difficult to measure T_e in the

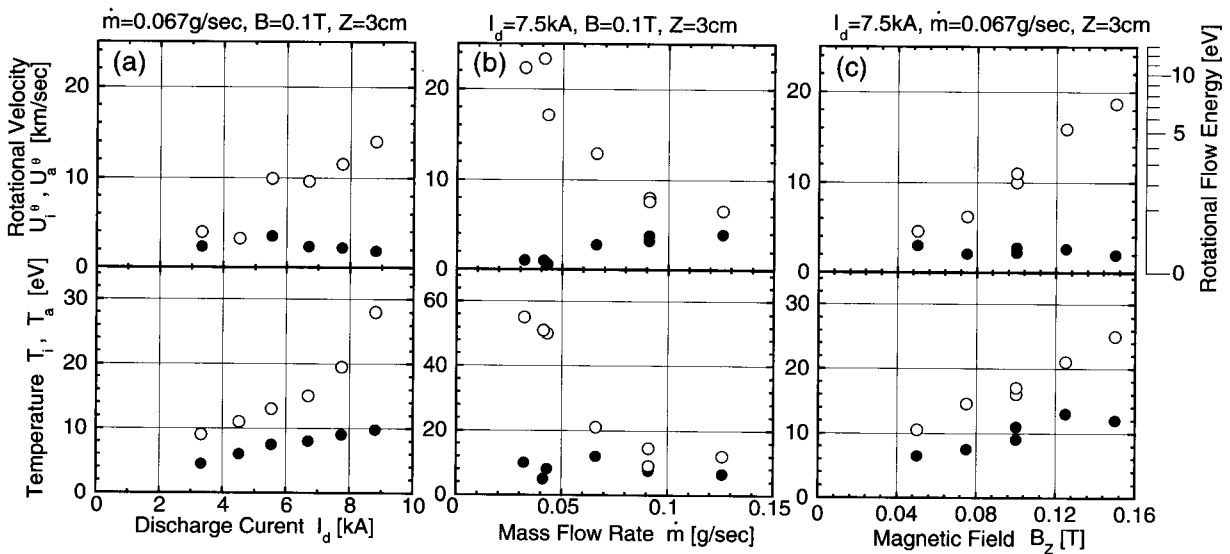


Fig. 2 Rotational velocities U_i^θ , U_a^θ and temperatures T_i , T_a as functions of (a) I_d , (b) \dot{m} and (c) B_z . Open and solid symbols are those obtained from HeII and HeI lines, respectively.

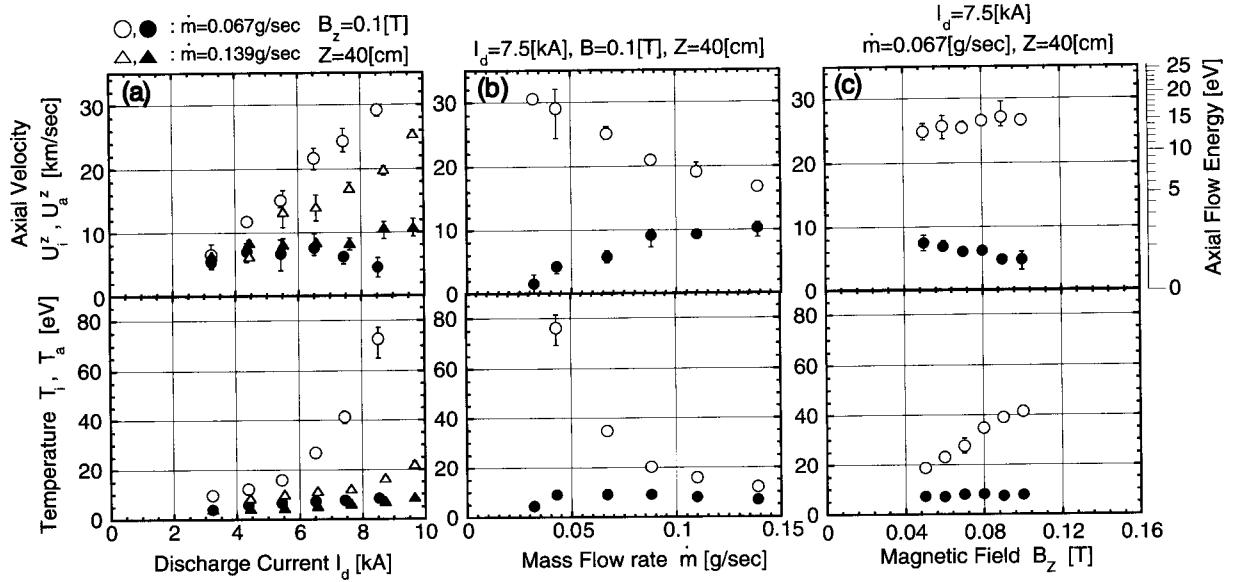


Fig. 3 Axial velocities U_i^z, U_a^z and temperatures T_i, T_a as functions of (a) I_d , (b) \dot{m} and (c) B_z . Symbols are the same as those in Fig. 2.

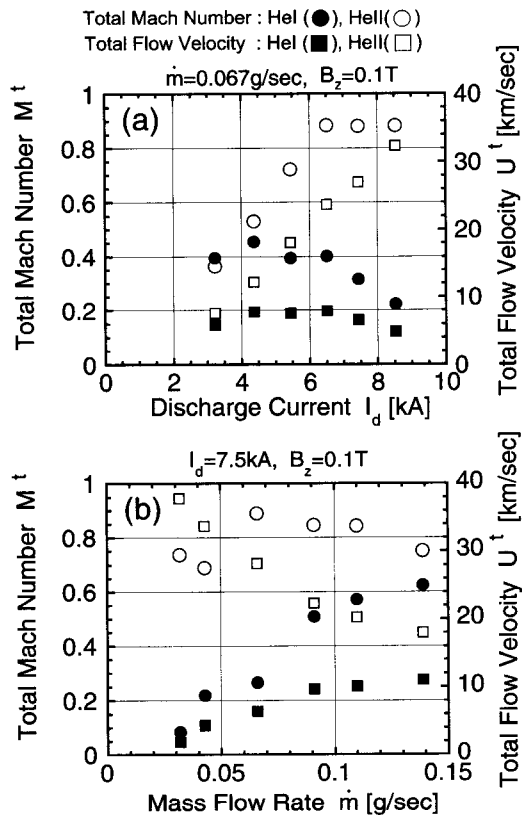


Fig. 4 Total velocities U_i^t (open squares) and total Mach number M_i^t (open circles) of He ions as functions of (a) I_d and (b) \dot{m} . Those of neutral atoms are plotted as solid ones.

outlet region of MPD arcjet. In the downstream region of the plasma flow T_e is measured by electrostatic probe and obtained 5–10eV. Though T_e is probably lower than T_i , it is assumed that T_e equals to T_i in the calculation of M_i^t . The same dependence of He atoms is also plotted in the figure.

The total ion velocity increases with the increase in the current and with the decrease in the mass flow rates. As is shown in the figure the total Mach number tends to saturate at 1 in the region of higher current and lower mass flow rate. When M_i^t is saturated, T_i strongly increases as shown in Fig. 2 and Fig. 3. These saturation phenomena of M_i^t seems to be related to the occurrence of a shock wave.

A radial profile of space potential $\phi_s(r)$ can be estimated from the obtained profile of U_i^θ in the rotating plasma. The radial force-balance equation for a plasma rotating with the azimuthally-rotational velocity U_θ is given by

$$Mn \frac{U_\theta^2}{r} - \frac{\partial p}{\partial r} + J_\theta B_z - J_z B_\theta = 0 \quad (3)$$

Here, M is an ion mass and $p = p_i + p_e$ is a total pressure. A generalized Ohm's law with the assumption of negligible resistivity can be expressed as,

$$en(E_r + U_\theta B_z) - J_\theta B_z + J_z B_\theta + \frac{\partial p_e}{\partial r} = 0 \quad (4)$$

Then the rotational velocity U_θ is obtained as

$$U_\theta = -\frac{E_r}{B_z} + \frac{T_i}{eB_z} \frac{\partial \ln n}{\partial r} - \frac{MU_\theta^2}{reB_z} \quad (5)$$

The rotational velocity is composed of three terms, $E \times B$ drift, diamagnetic drift and centrifugal force drift.

When the density profile $n(r)$ is assumed to be gaussian, $n(r) = n_0 \exp(-r^2/r_0^2)$, the equation can be normalized with non-dimensional variables, $X = \omega/\Omega_i$, $Y = \omega_{E \times B}/\Omega_i$ and $\Gamma = (\rho_i/r_0)^2$,

$$X^2 + X = Y - \Gamma \quad (6)$$

Here, $\omega = U_\theta/r$ is an angular frequency of the rotation, $\omega_{E \times B} = -E_r/rB_z$ is that of $E \times B$ drift, $\Omega_i = eB_z/M$ is ion

cyclotron angular frequency and $\rho_i = \sqrt{2MT_i}/eB_z$ is ion cyclotron radius. As the $E \times B$ drift term dominates the rotational velocity in eq.(5), the plasma rotates in the same direction as that of the $E \times B$ drift. Using the experimental result shown in Fig. 1, radial profiles of $E_r(r)$ and $\phi_s(r)$ in the rotating plasma are calculated and are shown in Fig. 5. The derived potential profile in the core region is almost parabolic. The ratio of the three terms in eq.(5) is 2:1:0.35 in this case.

The increase of rotational velocity with the increase of B_z , as appeared in Fig. 2(c), is mainly due to the increase of E_r , which has been confirmed by other experiments.

4. Conclusion

Flow velocity and temperature of an axially-magnetized MPD arcjet plasma are measured by spectroscopy in the HITOP device. With the externally-applied magnetic field B_z , the plasma is accelerated not only axially by $J_r \times B_\theta$ force, but azimuthally by $J_r \times B_z$ force, where J_r is radial discharge current and B_θ is self-induced azimuthal magnetic field.

The axial and rotational velocities and ion and atom temperatures are measured by the Doppler shift and broadening of the HeII and HeI lines.

The axial and rotational velocities increase with the increase in discharge current and with the decrease in mass flow rates. It is noted that the rotational velocity increases with the applied magnetic field strength, while the axial velocity is independent of it. Total ion velocity and Mach number are calculated and the Mach number of the flow tends to saturate at near 1 in the operation regions of higher discharge current and lower mass flow rate. The strong increase of T_i is observed in these operation regions.

Radial profile of space potential is evaluated from the experimental data of rotational velocity. The potential profile in the core region is parabolic corresponding to the rigid-body rotation.

5. Acknowledgments

This work was supported in part by a Grant-in-Aid for Scientific Research from the Ministry of Education, Science and Culture of Japan. Part of this work was carried out under the Cooperative Research Project Program of the Research Institute of Electrical Communication, Tohoku University.

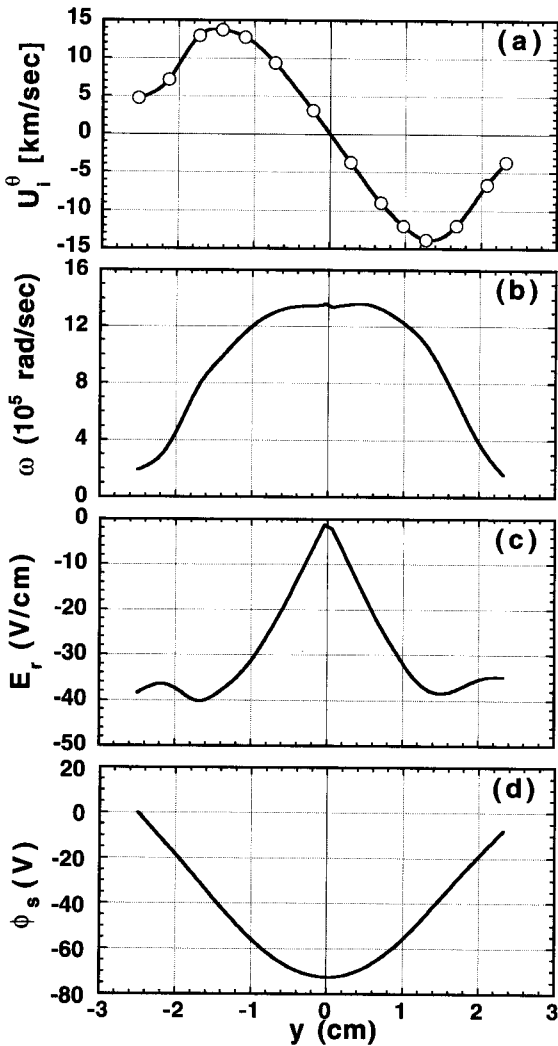


Fig. 5 Radial profiles of (a) U_θ^0 , (b) ω , (c) E_r , and (d) ϕ_s .

References

- [1] S.M. Mahajan and Z. Yoshida, *Phys. Rev. Lett.*, **81**, 4863 (1998).
- [2] R.G. Jahn, *Physics of Electric Propulsion, McGraw-Hill press*, (1968).
- [3] M. Sasoh and Y. Arakawa, *J. of Propulsion and Power* **11**, 351 (1995).
- [4] A. Ando *et al.*, *Proc. of the Int. Conference on Plasma Physics (ICPP96, Nagoya)* **1**, 2014 (1996).
- [5] A. Ando *et al.*, *Proc. of 25th EPS and Int. Congress on Plasma Physics (ICPP98, Praha)* **22C**, 51 (1998).
- [6] M. Inutake *et al.*, *Proc. of 26th International Electric Propulsion Conference (IEPC-99-175, Kokura)* **2**, 1010 (1999).